



# Bioprospecting solid binding polypeptides for lithium ion battery cathode materials

Evgenia A. Barannikova, Scott J. Riley, and Mark A. Allen<sup>a)</sup>

Department of Chemistry and Biochemistry, University of Maryland, Baltimore County, Baltimore, Maryland 21250

(Received 29 May 2019; accepted 26 September 2019; published 15 October 2019)

Biotemplating presents a promising approach to improve the performance of inorganic materials via specific control over morphology, crystal structure, and the size of particles during synthesis and assembly. Among other biotemplates, solid binding polypeptides (SBPs) isolated for the material of interest provide high binding affinity and selectivity due to distinct combinations of functional groups found in amino acids. Nanomaterials assembled and synthesized with SBPs have found widespread applications from drug delivery to catalysis and energy storage due to their improved properties. In this study, the authors describe the identification of SBPs for binding to Li-ion battery cathode materials  $\text{LiCoPO}_4$ ,  $\text{LiMn}_{1.5}\text{Ni}_{0.5}\text{O}_4$ , and  $\text{LiMn}_2\text{O}_4$ , which all have potential for improvement toward their theoretical values. The binding affinity of isolated peptides was assessed via phage binding assays and confirmed with electron microscopy in order to select for potential biotemplates. The authors demonstrate ten binding peptides for each material and analyze the sequences for enrichment in specific amino acids toward each structure (olivine and spinel oxide), as well as the test for specificity of selected sequences. In further studies, the authors believe that the isolated SBPs will serve as a template for synthesis and aid in assembly of cathode materials resulting in improved electrochemical properties for Li-ion batteries. *Published by the AVS.*

<https://doi.org/10.11116/1.5111735>

## I. INTRODUCTION

Lithium ion batteries are nearly ubiquitous for personal portable electronics; yet, limitations remain to expand their use outside of small electronic devices due to issues involving safety and power performance.<sup>1–3</sup> Safety concerns, in particular, continue to prevent the advancement of larger form factor batteries capable of packing the same energy density available to lithium ion technology used in portable devices. One of the largest safety concerns arises from the high internal resistance inside the battery electrode caused by the intrinsically poor electrical conductivity of electroactive particles.<sup>4–6</sup> Materials exhibiting a high internal resistance heat up when they are forced to transport electrons through the particles, which happens in Li-ion batteries when they are charged or discharged rapidly. This heat generated inside the electrode causes damage and decay to organic electrolyte and diminishes battery electrode performance. In extreme situations, the battery may undergo thermal runaway resulting in catastrophic failure.<sup>3–5</sup> Several techniques have been employed in order to ameliorate an electrode's internal resistance including the addition of better conductive additives and decreasing the path that electrons have to travel by making nanosized electroactive particles.<sup>7,8</sup> Together, these two methods improve ionic and electronic conductivity, mitigating some of the resistance and decreasing the heat built up inside the battery, which also allow for higher power performance and greater theoretical capacity to be achieved. Developing new synthetic methodologies as well as methods

for increasing the electrical connectivity remains an important endeavor toward better performing nanomaterials.

Making materials through a biotemplated approach has resulted in materials with improved properties and serves as a reasonable and environmentally benign method of controlling particle size as well as morphology.<sup>9–11</sup> Nature has a diverse toolkit that contains complex molecules including nucleic acid polymers, lipids, polysaccharides, and proteins, and each of these has been used for direct applications in nanotechnology including sensors and electronic devices.<sup>10–13</sup> Among these macromolecules, proteins represent nature's most diverse polymer with a range of functionalities determined by 20 genetically encoded natural building blocks. Many such proteins contain functional groups that are responsible for the interactions between hard inorganic materials and soft biological molecules and enable the biomimetic mineralization of hard shells, biogenic silica, and magnetic particles.<sup>14–17</sup> In addition to natural minerals, it is possible to use proteins for the synthesis and assembly of technologically relevant inorganic materials with improved characteristics.<sup>18–24</sup>

While biotemplated and biotethered materials have served as functional sensors among other applications for many years,<sup>25,26</sup> battery electrode materials are one of the first technologically relevant materials that were incorporated into a functional device prepared through a biotemplated approach. Pioneering work utilizing biological molecules to synthesize electrode particles began in 2006, when electroactive materials were precipitated on the surface of a nonspecific bacteriophage template.<sup>27</sup> Since then, more work has been performed on the application of biotemplating for the lithium ion batteries,<sup>19,27–32</sup> which culminated in developing

<sup>a)</sup>Electronic mail: allenm@umbc.edu

multifunctional bacteriophage serving as a bridge between electroactive particles and conducting additives.<sup>28</sup> In these studies, the biotemplate accounted for a large mass of inactive material inside the battery electrodes, yet only a small component of the biomolecules was necessary to impart functionality. Early success in biotemplating battery materials using larger proteins opened up future applications for short solid binding polypeptides (SBPs) that can serve as a biotemplate both for synthesizing electrode particles and for biotethering conducting additives to the particles, resulting in safer and higher power biotemplated batteries.

There are several methods available for the identification of functional polypeptides; however, the most frequently employed technique is based on M13 bacteriophage.<sup>33,34</sup> The earliest phage display studies were performed to identify polypeptides bound specifically to immunogenic toxins or viruses.<sup>35,36</sup> While these medically relevant targets remain important substrates for phage display, it has become apparent that phage display libraries can be utilized to find polypeptides with a high binding affinity to inorganic substrates. Once these SBPs are identified, they can be employed to improve synthesis and hierarchical assembly for complex inorganic materials. The earliest work toward this goal was identifying SBPs that bound to the mixed valence iron oxide magnetite.<sup>37,38</sup> Since this seminal work, several materials have been successfully pursued for targets using a randomized phage display library including noble metals (Ag, Au),<sup>39,40</sup> metal oxides (SiO<sub>2</sub>, TiO<sub>2</sub>, ZnO),<sup>41–43</sup> semiconductive (GaAs, InP, ZnS, CdS),<sup>20,44,45</sup> magnetic (FePt, CoPt),<sup>21</sup> and other technologically relevant materials.

In this report, we present the use of phage display to identify short 12mer polypeptides that bind to various lithium ion battery cathode materials, specifically LiCoPO<sub>4</sub>, LiMn<sub>2</sub>O<sub>4</sub>, and LiMn<sub>1.5</sub>Ni<sub>0.5</sub>O<sub>4</sub>. The binding affinities of isolated phage have been quantitatively characterized through phage binding assays. Electron microscopy was used to obtain images that indicate the colocalization of phage presenting SBPs and particles. Analysis of the sequences was performed to characterize enrichment of certain binding motifs, which indicated that the chemical functionalities present within the sequence are important in defining the binding characteristics. To our knowledge, this is the first work on the identification of SBPs that bind specifically to complex battery cathode particles.

## II. EXPERIMENT

### A. Materials and reagents

The Ph.D.<sup>TM</sup>-12 Phage Display Peptide Library kit was purchased from New England BioLabs<sup>®</sup> (NEB). Lithium manganese nickel oxide (LiMn<sub>1.5</sub>Ni<sub>0.5</sub>O<sub>4</sub>, Nanomyte<sup>®</sup> SP-10, LMNO) and lithium manganese oxide (LiMn<sub>2</sub>O<sub>4</sub>, Nanomyte BE-30, LMO) were purchased from NEI Corporation<sup>TM</sup>, and lithium cobalt phosphate (LiCoPO<sub>4</sub>, LCP) was received from Sigma-Aldrich. All other reagents were purchased from VWR Life Sciences.

### B. Phage display method optimization

Phage display was performed at a range of pH and ionic strengths depending on the stringency of an elution and the type of particles that serve as a binding target. Buffers used were always 10 mM in concentration [phosphate (Li<sub>x</sub>H<sub>3-x</sub>PO<sub>4</sub>), borate (Li<sub>x</sub>H<sub>3-x</sub>BO<sub>3</sub>), or tris(hydroxymethyl)aminomethane (tris) with respective pH values adjusted with LiOH]. Phage library (10 µl) was diluted into buffer (990 µl) and a negative selection was performed against all surfaces that phage would be exposed to during biopanning. After negative selection, a defined mass (10–30 mg) of material of interest, prewashed with buffer, was added and incubated for 1 h at room temperature with continuous agitation using an orbital shaker. Biopanning involved washing particles with buffer, isolating them by centrifugation (17 000 rcf, 2 min), and resuspending in elution buffer containing a surfactant (Tween-20) between 0.2% and 0.6% v/v. Following surfactant elution of 0.8% Tween, the material was washed with a low pH buffer (0.2M Glycine-HCl, pH 2.2 + 1 mg/ml BSA). Phage eluted in the final wash as well as the phage that remain bound to particles were amplified by *E. coli* ER2738 infection. After the third round of biopanning, the samples were titered<sup>46</sup> and individual plaques were isolated for DNA sequencing. Phage DNA was purified using the Zippy<sup>TM</sup> Plasmid Miniprep Kit (Zymo Research, USA), and 96III primer (NEB) was added for sequencing (Genewiz<sup>®</sup>).

### C. Determining binding factor of specific phage sequences

A defined mass (10–30 mg) of target material of interest was measured and washed with buffer several times until the pH was stable. Phage stock was diluted into buffer to an estimated concentration of  $1 \times 10^8$ – $1 \times 10^9$  pfu/ml. An aliquot (10 µl) was saved for titering to determine the actual phage concentration (input). Phage were incubated with the material for 1 h at room temperature (20–22 °C) with constant agitation. Materials were washed ten times with buffer containing 0.5% v/v Tween-20 to remove weakly bound phage. A final elution with low pH buffer (0.2M Glycine-HCl, pH 2.2 + 1 mg/ml BSA) was performed followed by the addition of neutralization buffer (1M Tris-HCl pH 9.1, 150 µl). The supernatant was titered to determine the concentration of tightly bound phage (output). A binding factor was determined by a ratio of the output phage concentration with respect to the input phage concentration of a specific phage mutant normalized to the binding ratio (output/input) for wild-type phage lacking a binding insert.

### D. Specificity characterization

LMO and LMNO share a spinel oxide structure with space group *Fd* $\bar{3}m$ . Phage specificity was evaluated for the two similar oxides using selectivity and cross-binding analysis. Selectivity experiments were performed similar to output/input analysis, wherein phage particles with the highest binding factor for each material (LMO1 and LMNO1,  $2 \times 10^9$  pfu/ml) were added to both materials followed by extensive washing with Tween detergent solution and pH 2.2 Glycine-HCl

elution. Phage remaining on the material were eluted with 1 ml of *E. coli* and titered followed by DNA sequencing to determine the frequency of each phage type binding to either LMNO or LMO. Cross-binding analysis was performed similarly, however, rather than combining phage to determine which appears more frequently, the phage were added individually to each material, washed extensively, and eluted with 1 ml of *E. coli*. Phage concentrations were determined by titration.

### E. Transmission electron microscopy

Samples (10  $\mu$ l) that were either particles alone (control) or particles with phage ( $1 \times 10^8$  pfu) were placed on a copper grid (300 mesh formvar/carbon, Electron Microscopy Sciences) and allowed to sit for 10 min. Samples were wicked, washed with water, dried, and imaged using a Morgagni M268, 100 kV with a Gatan Orius CCD camera (FEI, 100 kV, Keith R. Porter Imaging Facility, UMBC).

### F. Scanning electron microscopy

Scanning electron microscopy (SEM) samples were prepared via a multistep process in which LCP particles alone (<2000 nm) or particles with phage ( $1 \times 10^8$  pfu) were cast onto aluminum tape (Ted Pella) which was attached to an SEM sample holder by conducting adhesive. SEM images were obtained using a Nova NanoSEM 450 (FEI, EDT detector, EV: 10–15 kV, working distance 5.0 mm, spot size 3.0, UMBC NanoImaging Facility).

## III. RESULTS AND DISCUSSION

### A. Phage display for cathode materials

Lithium ion battery materials LiCoPO<sub>4</sub> (LCP), LiMn<sub>1.5</sub>Ni<sub>0.5</sub>O<sub>4</sub> (LMNO), and LiMn<sub>2</sub>O<sub>4</sub> (LMO) were chosen as targets for phage display. Each of these materials has a high theoretical energy density which makes them valuable targets for battery electrodes (Table I).<sup>47–50</sup> While these three electroactive materials offer high electrochemical potential, their full theoretical capacities have not yet been realized. The performance of these electroactive particles may be improved through biotemplating. In order to enhance the empirical performance of these electroactive materials, we present SBPs that have been identified, discuss the characteristics of these peptides, and quantitatively assess relative binding affinities.

Phage display was performed for each of the battery electrode particles in order to identify SBPs. LCP, LMO, and LMNO particle slurries were exposed to a library of M13

bacteriophage followed by biopanning. Biopanning requires the exposure of particles to aqueous buffer in the presence of the phage library. This is relevant considering that lithiated battery electrodes often exchange Li<sup>+</sup> present in the particle with H<sup>+</sup> in the aqueous buffer causing the material to become delithiated and for the pH of the solution to increase.<sup>51,52</sup> Changes in pH were monitored and did indicate that delithiation happened for the oxide materials but was not apparent for LCP (verified by inductively coupled plasma mass spectrometry). In all cases, it was found that Li<sup>+</sup>/H<sup>+</sup> exchange was controllable if an excess of Li<sup>+</sup> was added to all buffers.

In all biopanning experiments, a negative selection was performed in order to eliminate nonspecific phage. Negative selection involved exposing the phage display library to several surfaces including polypropylene cups, pipet tips, and centrifuge tubes to eliminate these phage from the library. Following negative selection, biopanning experiments were performed (Fig. S1).<sup>57</sup> Several elution conditions were used to eliminate nonspecific phage from particles; these included surfactant washes, low and high pH (pH = 2 or 9) elutions, and a final elution from material using an *E. coli* wash. Each of these elution steps was chosen in order to sample the different charge states of the cathode particles as well as the different ways that proteins can interact with target materials. The charged states of particles were determined through zeta potential measurements, indicating that the particles had an overall positive charge at very low pH (pH = 2) and a negative surface potential at all higher pH levels (Fig. S2).<sup>57</sup> The surfactant (Tween-20®) was used in elution buffers with the aim to remove phage that were weakly bound through hydrophobic interactions with target materials. Collectively, these many wash steps make up the iterative process of biopanning. After three rounds of biopanning, the original library diversity was decreased from around  $1 \times 10^9$  variable 12mer polypeptide sequences down to between 30 and 40 potential sequences (Table S1).<sup>57</sup> Phage binding analysis in the form of output/input studies was valuable in selecting the most relevant binding sequences for further analysis.

### B. Phage binding analysis

After three rounds of biopanning, several sequences were identified that were likely to have some specific interactions with the intended electrode particle targets. Some of the sequences appeared in biopanning experiments multiple times which could indicate that these sequences had a stronger interaction with particles. In order to quantitatively assess the relative affinity from each sequence for its target, an output/input binding assay was performed (Fig. 1).<sup>53,54</sup>

The goal of an output/input assay is to identify phage with higher binding affinity to target particles compared to nonspecific wild-type phage that present no random peptide insert on its pIII minor coat protein. Phage (both phage identified through phage display and wild-type M13) were amplified in *E. coli* and diluted to a similar concentration ( $1 \times 10^9$  plaque forming units per milliliter, pfu/ml). During the assay, control

TABLE I. Electrochemical properties of selected cathode materials.

Material	Potential vs Li/Li <sup>+</sup> (V)	Theoretical capacity (mA h/g)	Theoretical energy density (W h/kg)
LCP	4.8	167	801
LMNO	4.7	147	691
LMO	4.0	148	607

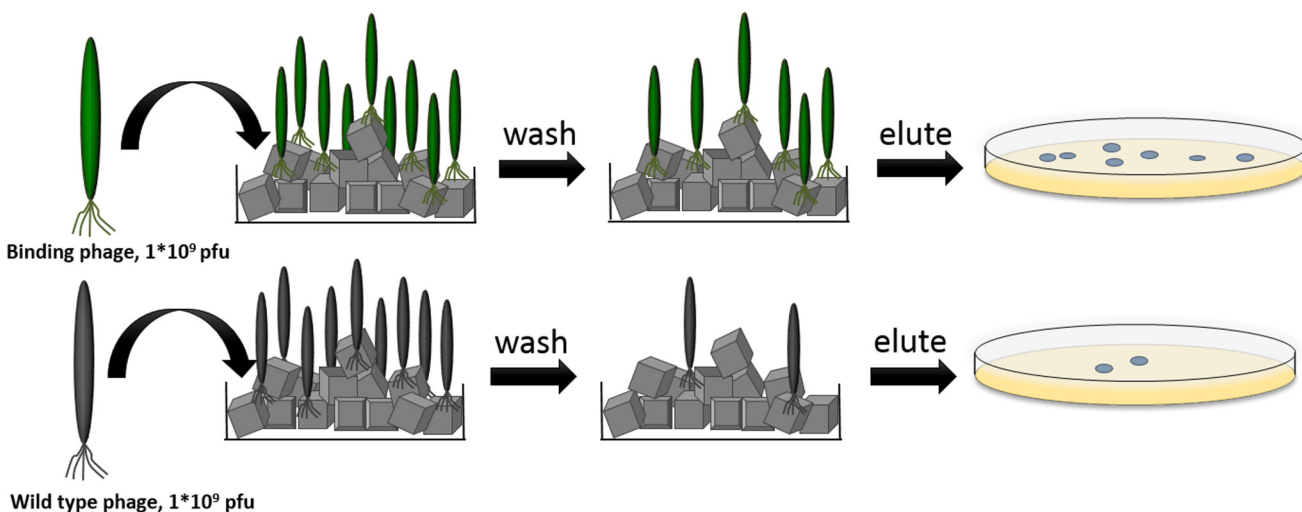


FIG. 1. Phage relative binding assay.

phage (wild-type M13) and material specific phage identified through phage display were exposed to particles and subsequently washed thoroughly to remove unbound or weakly bound phage. After washing the particles ten times with buffer containing surfactant, the phage were finally eluted using a low pH and high salt buffer. This elution step resulted in output phage; the concentrations of input (initial phage stock) and output phage were determined through titering.<sup>46</sup> The binding ratio is a normalized ratio of output phage that remained bound to particles throughout all 10 washing steps to input phage concentration relative to this same ratio determined for nonspecific wild-type phage. A binding ratio that is lower than 1 indicates an affinity that is weaker than wild-type M13 phage; a binding ratio higher than 1 indicates that the peptide insert on phage has some specific interaction with particles that is greater than the nonspecific interactions of wild-type M13.

Several sequences for each material were analyzed through output/input phage binding analysis (Table II). These sequences are presented in order of the highest binding factor in comparison to wild-type phage. The first nine sequences in each table have a binding factor that is higher than wild type, the tenth sequence in each table is presented specifically because it has a binding factor that is less than one in comparison to wild-type phage despite the fact that it was identified multiple times through biopanning (Table II, frequency column). Having a low binding factor indicates weaker interactions than the non-specific interactions of wild-type phage for each material. The fact that the tenth sequence remains after performing biopanning may be the result of amplification bias or some other factor that is not dependent on material binding.<sup>55</sup>

Peptide sequences identified for LCP did not seem to cluster into any clear groups. Isoelectric points (pIs) ranged from 3 to 11 and the frequency of how many times each sequence appeared did not seem to correlate strongly with the binding affinity (Table IIA). Sequence LCP1 (FNFPVTEFDHVL) had the highest binding factor followed by three mutants that all had similar binding factors and pIs. Sequence LCP10 (SAAYLAVIDTSS) had the lowest binding affinity (<wild

type) and also the lowest pI even though it was identified five times and in different biopanning experiments. The top three sequences for LCP were compared further using electron microscopy.

In contrast with LCP, most of the peptide sequences identified for LMNO (Table IIB) have pIs between 5 and 8. A notable exception, LMNO10 (ISAKTHTSPPRM), was isolated several times over different rounds of phage display, binds less tightly than wild-type phage, and has a very high pI (11.5). Sequence LMNO1 (SSNPTVYAPPLG) was isolated twice in different rounds of phage display, and it was found to bind five-fold stronger than wild-type phage. Other sequences that were isolated multiple times did not have as high binding affinity as LMNO1. Nearly all the sequences identified for LMO (Table IIC) have high isoelectric points (>9.5) and little sequence similarity to LMNO sequences. The presence of positively charged amino acid residues in each LMO sequence could be indicative of electrostatic interactions with the metal oxide surface of the material. The sequence LMO1 (LSQQPTAQLMRA) had the highest binding affinity based on the output/input binding ratio.

Sequence analysis of SBPs for all three materials was highly heterogeneous and offered no clear trend in isoelectric point. These observations indicate that the pI of a peptide alone cannot serve as a useful way for determining superior binding to its target material making other techniques necessary to determine binding specificity. Therefore, binding assays were necessary in order to quantify binding affinity for target particles.

### C. Multiplication factor for amino acids

The phage library itself can bias the results of phage display; not every amino acid is represented in equal amounts across the phage library and some amino acids are over-represented, subsequently not contributing to specific interactions with particles. Performing biopanning for any material will result in an enrichment of relevant amino acids that

TABLE II. Binding factors of isolated phage mutants containing SBPs for target materials.

No.	Sequence												BF	pI	Frequency
<b>(A) Peptide sequences identified for LCP</b>															
LCP1	F	N	F	P	V	T	E	F	D	H	V	L	9.3	4.16	1
LCP2	Q	V	N	G	L	G	E	R	S	Q	Q	M	6.0	6.76	7
LCP3	Y	Y	S	A	G	I	G	R	V	A	Y	D	4.9	6.49	1
LCP4	W	T	S	P	W	P	S	E	L	R	Y	V	4.7	6.76	3
LCP5	D	G	R	R	N	I	S	F	R	P	G	Y	3.7	11.04	1
LCP6	M	P	Y	M	N	V	M	Q	W	D	G	P	3.5	3.37	1
LCP7	H	T	P	A	A	T	L	H	P	V	F	L	2.6	7.52	3
LCP8	I	S	R	A	N	L	M	M	N	T	Y	D	2.0	6.50	1
LCP9	G	N	N	P	L	H	V	H	H	D	K	R	1.0	9.07	1
LCP10	S	A	A	Y	L	A	V	I	D	T	S	S	0.6	3.37	5
<b>(B) Peptide sequences identified for LMNO</b>															
LMNO1	S	S	N	P	T	V	Y	A	P	P	L	G	5.0	5.92	2
LMNO2	H	G	T	F	H	T	F	S	P	V	T	M	2.3	7.94	1
LMNO3	V	H	C	S	T	T	T	M	N	T	P	R	2.3	8.93	3
LMNO4	Q	V	P	L	S	A	Q	A	W	E	S	H	1.8	5.17	8
LMNO5	S	T	H	P	P	L	P	E	T	H	P	I	1.7	6.03	1
LMNO6	S	L	S	L	N	H	A	I	M	K	P	S	1.5	10.04	1
LMNO7	H	H	S	S	Y	V	A	S	S	T	I	H	1.5	7.97	1
LMNO8	H	I	S	L	S	L	A	R	D	L	E	M	1.4	5.25	1
LMNO9	F	T	S	L	T	D	R	T	S	Y	Y	M	1.3	6.63	1
LMN10	I	S	A	K	T	H	T	S	P	P	R	M	0.8	11.54	5
<b>(C) Peptide sequences identified for LMO</b>															
LMO1	L	S	Q	Q	P	T	A	Q	L	M	R	A	2.7	11.03	1
LMO2	S	T	S	L	I	G	V	V	A	P	H	M	2.1	7.79	1
LMO3	T	G	S	K	S	V	H	E	N	R	P	V	2.1	10.04	1
LMO4	L	I	S	P	S	A	P	T	K	P	N	V	1.7	10.04	1
LMO5	M	P	H	P	V	G	N	H	S	K	R	V	1.6	11.54	1
LMO6	H	D	P	S	N	K	W	R	L	L	A	M	1.6	10.04	1
LMO7	A	E	M	K	T	S	A	S	R	L	H	Y	1.5	9.7	1
LMO8	T	I	T	S	S	L	R	P	T	T	L	H	1.4	11.03	2
LMO9	S	T	V	Y	H	T	T	P	Y	H	N	R	1.4	9.58	1
LMO10	Y	L	I	P	V	R	S	L	S	M	S	T	0.6	9.82	2

deviate from the diversity of the original library. Table III shows multiplication factors that describe the distribution of 20 genetically encoded amino acids present in the Ph.D.-12® phage display library with respect to identified SBPs. A multiplication factor was calculated as the ratio between the percent of amino acid found for the target material relative to the abundance of that amino acid in the Ph.D.-12 peptide library (New England Biolabs). Amino acids found in high or low abundance are defined as those that have the multiplication factor higher than 1.25 or lower than 0.75, respectively.<sup>56</sup>

Analysis of the sequences presented in Table II compared to the amino acid pool in the library indicates that certain amino acids are over-represented in the pool of SBPs and some are under-represented (Table III). Specifically, tyrosine, phenylalanine, methionine, and asparagine are over-represented in the LCP binding sequences and lysine is under-represented. This is indicative that lysine with a positive charge is not necessary for binding; however, the amide functionality on asparagine does seem to be relevant. As an example, the LCP2 (QVNGLGERSQQM) sequence, which has a binding factor of 6.7, is highly enriched in amide

containing amino acids. The peptide sequences isolated for LMNO and LMO are collectively enriched in threonine and histidine, which are prevalent in binding sequences for several metal oxides.<sup>56</sup> In addition, sequences found for LMNO featured high levels of serine and are depleted in other polar amino acids such as asparagine and glutamine and negatively charged aspartic acid. Sequences for LMO are enriched in positively charged lysine residues and depleted in negatively charged glutamic and aspartic acids, which is why the pI of the LMO SBPs is considerably higher than those for LMNO. It appears that peptide affinity for LMO is largely electrostatic since the particles are negatively charged at the pH levels that the display is performed under (Fig. S2).<sup>57</sup> The strongest binding sequences LMNO1 (SSNPTVYAPPLG) and LMO1 (LSQQPTAQLMRA) are abundant in polar amino acids, which can form hydrogen bonds with metal oxides.

#### D. Binding specificity

LMO and LMNO have similar crystal structures (both are spinel oxides with an  $Fd\bar{3}m$  space group) and also have

TABLE III. Amino acid frequency of isolated binding peptides found for each material.

Amino acids	Multiplication factor		
	LCP	LMNO	LMO
G	1.15	0.31	0.43
A	0.90	0.86	0.79
V	1.23	0.60	1.23
L	0.75	0.92	1.03
I	0.98	1.07	0.98
P	0.93	1.46	1.23
S	0.67	1.38	1.26
T	0.64	1.86	1.39
Y	1.85	1.01	0.93
D	1.27	0.40	0.18
E	0.81	0.88	0.54
N	1.48	0.61	0.93
Q	0.85	0.23	0.64
R	1.17	0.64	1.17
K	0.36	0.79	1.81
H	1.09	1.78	1.63
F	1.54	0.67	0.00
W	1.09	0.40	0.36
M	1.61	1.76	1.61
C	0.00	0.61	0.00

nearly identical surface potentials at the pH of binding experiments (Fig. S2).<sup>57</sup> It would be expected that SBPs for LMNO and LMO would have overlapping properties, but the strongest binding sequences for LMNO and LMO were very different from each other. This may indicate that these peptides bind to different crystal faces or may also indicate that sequences for LMO bind primarily through electrostatic interactions while LMNO may be more specific to the material surface. To assess the selectivity and specificity of isolated phage mutants, phage presenting LMO1 and LMNO1 were screened against both target materials in two separate experiments. In the selectivity assay, phage presenting LMO1 and LMNO1 were diluted to equal concentration ( $2 \times 10^9$  pfu/ml), mixed together, and added to each material (LMO and LMNO, 10 mg). These samples were allowed to interact for 1 h, washed extensively with the detergent solution and eluted with *E. coli*. Phage were titered, and DNA sequencing of blue plaques was performed to determine which phage remained bound to the different oxide particles. The results of DNA sequencing indicated that sequence LMO1 appeared for LMO 90% of the time (nine out of ten sequences). However, the same sequence LMO1 was also dominant on nontarget material LMNO (seven out of eight sequences), which indicates that LMO1 is a nonspecific binder and that it binds to both oxides better than the

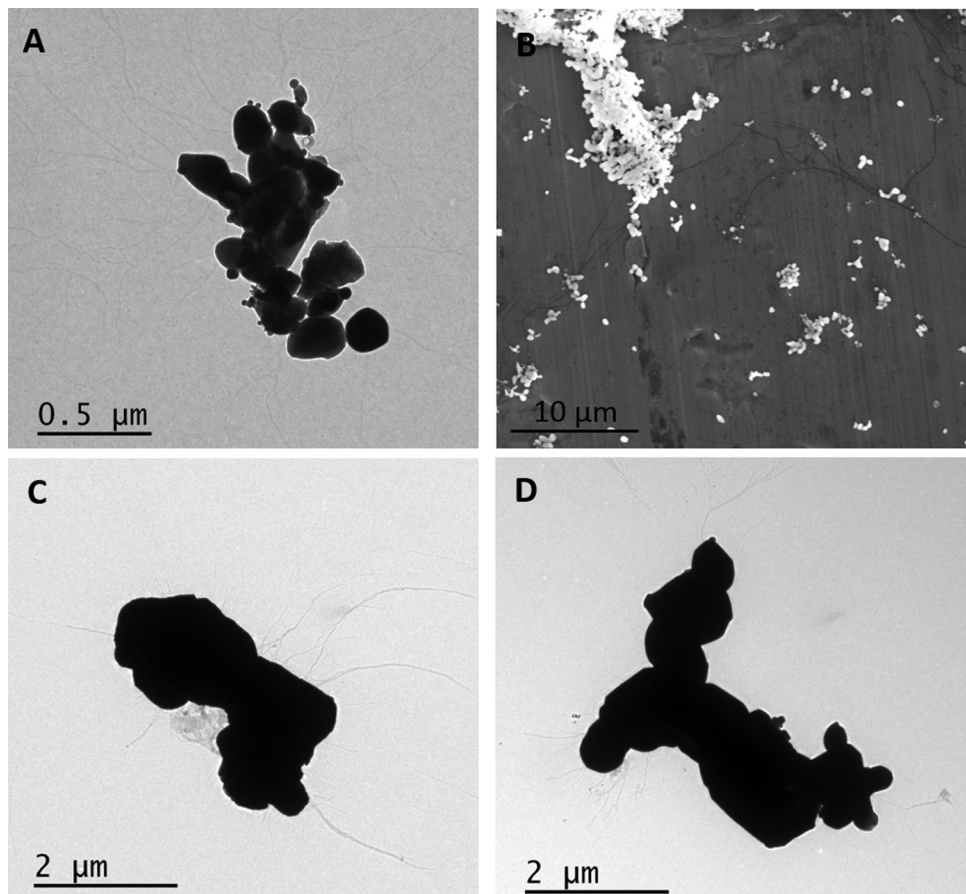


FIG. 2. Electron microscopy images of isolates phage bound to the target material: (a) TEM image of LCP2 phage bound to LCP; (b) SEM image of LCP2 bound to LCP; (c) LMNO1 phage bound to LMNO; (d) LMO1 phage bound to LMO.

LMNO<sub>1</sub> sequence. LMO<sub>1</sub> may be a general oxide binding polypeptide that binds through electrostatic interactions. Cross-binding studies were completed to confirm the specificity of binding. In this experiment, LMO<sub>1</sub> phage were added to both LMO and LMNO particles, incubated for an hour followed by extensive washing. Titering of each material indicated that LMO<sub>1</sub> bound similarly to both materials. In contrast, cross-binding studies for LMNO<sub>1</sub> revealed that this sequence only remained bound to LMNO and no phage were identified still bound to LMO, indicating that LMNO<sub>1</sub> has a strong preference for LMNO. In conclusion, LMO<sub>1</sub> binds strongly to both oxides while LMNO<sub>1</sub> has specificity for LMNO.

### E. Electron microscopy

Transmission electron microscopy (TEM) was used as a qualitative assessment of phage binding to particles. The purpose of performing TEM was to verify that phage presenting specified sequences of peptides that were of interest for binding to their respective targets are actually colocalized with particles after thoroughly washing away unbound phage from the particles. In the TEM studies, phage presenting the strongest binding peptides were exposed to target materials prior to imaging.

Following the output/input analysis, three sequences with the highest binding factor (LCP1, LCP2, and LCP3) were explored using TEM. The imaging studies provided evidence of all three mutants binding to individual particles; however, the LCP2 sequence was present at a higher concentration surrounding particles compared to other sequences, indicating that it may have a higher binding affinity to the material [Fig. 2(a)]. This, coupled with the number of appearances of LCP2, establishes that LCP2 is the strongest binder identified. SEM was also utilized to visualize phage binding to LCP [Fig. 2(b)]. SEM provides the ability to use a larger portion of the sample with a wider field of view. Images were collected in order to support the findings of TEM and ensure that no bias was created during TEM sample preparation. Phage presenting the LCP2 sequence were visualized as extending off the LCP particles perpendicularly aligned.

TEM of phage presenting the highest binding factor LMNO<sub>1</sub> [Fig. 2(c)] and LMO<sub>1</sub> [Fig. 2(d)] sequences was confirmed to interact strongly with their respective particles. Control images of particles without phage (Fig. S3)<sup>57</sup> were not coated with biomolecules; however, when phage presenting the specified sequences were exposed to the material then phage are clearly visible as binding to particles in a manner consistent with peptides present on one end of the viruses as would be expected. SEM and TEM are useful tools that add support to quantitative methods like output/input studies for phage binding.

### IV. SUMMARY AND CONCLUSIONS

In this report, we have successfully demonstrated the utility of phage display technique toward the identification of SBPs for complex battery cathode materials, specifically LiCoPO<sub>4</sub>,

LiMn<sub>2</sub>O<sub>4</sub>, and LiMn<sub>1.5</sub>Ni<sub>0.5</sub>O<sub>4</sub>. These battery electrode materials are of interest due to their high theoretical potential and energy density and, yet, their performance has remained hindered by poor cyclability and rate capability.<sup>48–50</sup> After identifying several sequences for each material, the output/input binding analysis was used to quantify which sequences demonstrated the strongest binding affinities relative to the nonspecific binding of wild-type phage. Using multiplication factors based on the relative abundance of each amino acid present in the library, it was found that each material type allowed for certain amino acids to appear in much higher levels than in the native library. Of the nine strongest binding sequences, one particular sequence for each material was demonstrated to bind to particles of each substrate using TEM. Binding of phage presenting SBPs was also confirmed using SEM which corroborated data collected from TEM as well as provided a larger field of view for phage interacting with particles. The identification of these polypeptide sequences through phage display is the first step in developing individual solid binding polypeptide biotemplates, which will serve as a synthetic platform and as a tool for functionalizing battery electrode particles.

### ACKNOWLEDGMENTS

This work was supported by the UMBC Startup Funds and NIH/NIGMS Chemistry-Biology Interface Program grant (No. T32GM066706).

- <sup>1</sup>J. M. Tarascon and M. Armand, *Nature* **414**, 359 (2001).
- <sup>2</sup>D. Deng, *Energy Sci. Eng.* **3**, 385 (2015).
- <sup>3</sup>J. B. Goodenough and Y. Kim, *Chem. Mater.* **22**, 587 (2010).
- <sup>4</sup>A. Mauger and C. M. Julien, *Ionics* **23**, 1933 (2017).
- <sup>5</sup>H. Wang, E. Lara-Curzio, E. T. Rule, and C. S. Winchester, *J. Power Sources* **342**, 913 (2017).
- <sup>6</sup>M. S. Whittingham, *Chem. Rev.* **104**, 4271 (2004).
- <sup>7</sup>P. G. Bruce, B. Scrosati, and J.-M. Tarascon, *Angew. Chem. Int. Ed.* **47**, 2930 (2008).
- <sup>8</sup>Y. M. Sun, N. A. Liu, and Y. Cui, *Nat. Energy* **1**, 16071 (2016).
- <sup>9</sup>H. Zhou, T. X. Fan, and D. Zhang, *ChemSusChem* **4**, 1344 (2011).
- <sup>10</sup>D. S. Petrescu and A. S. Blum, *Wiley Interdiscip. Rev. Nanomed. Nanobiotechnol.* **10**, 29 (2018).
- <sup>11</sup>J. M. Galloway and S. S. Staniland, *J. Mater. Chem.* **22**, 12423 (2012).
- <sup>12</sup>J. Liu, S. Wagan, M. D. Morris, J. Taylor, and R. J. White, *Anal. Chem.* **86**, 11417 (2014).
- <sup>13</sup>F. H. Zang, S. Chu, K. Gerasopoulos, J. N. Culver, and R. Ghodssi, *Nanotechnology* **28**, 265301 (2017).
- <sup>14</sup>A. M. Belcher, X. H. Wu, R. J. Christensen, P. K. Hansma, G. D. Stucky, and D. E. Morse, *Nature* **381**, 56 (1996).
- <sup>15</sup>S. Mann, D. D. Archibald, J. M. Didymus, T. Douglas, B. R. Heywood, F. C. Meldrum, and N. J. Reeves, *Science* **261**, 1286 (1993).
- <sup>16</sup>M. Hildebrand, *Chem. Rev.* **108**, 4855 (2008).
- <sup>17</sup>T. Prozorov, *Semin. Cell Dev. Biol.* **46**, 36 (2015).
- <sup>18</sup>M. Uchida *et al.*, *Adv. Mater.* **19**, 1025 (2007).
- <sup>19</sup>X. Chen, K. Gerasopoulos, J. Guo, A. Brown, C. Wang, R. Ghodssi, and J. N. Culver, *ACS Nano* **4**, 5366 (2010).
- <sup>20</sup>C. E. Flynn, C. B. Mao, A. Hayhurst, J. L. Williams, G. Georgiou, B. Iverson, and A. M. Belcher, *J. Mater. Chem.* **13**, 2414 (2003).
- <sup>21</sup>C. B. Mao, D. J. Solis, B. D. Reiss, S. T. Kottmann, R. Y. Sweeney, A. Hayhurst, G. Georgiou, B. Iverson, and A. M. Belcher, *Science* **303**, 213 (2004).
- <sup>22</sup>S. Sotiropoulou, Y. Sierra-Sastre, S. S. Mark, and C. A. Batt, *Chem. Mater.* **20**, 821 (2008).
- <sup>23</sup>C. L. Chen and N. L. Rosi, *Angew. Chem. Int. Ed.* **49**, 1924 (2010).

- <sup>24</sup>M. B. Dickerson, K. H. Sandhage, and R. R. Naik, *Chem. Rev.* **108**, 4935 (2008).
- <sup>25</sup>C. A. Mirkin, R. L. Letsinger, R. C. Mucic, and J. J. Storhoff, *Nature* **382**, 607 (1996).
- <sup>26</sup>A. P. Alivisatos, *Science* **271**, 933 (1996).
- <sup>27</sup>K. T. Nam, D. W. Kim, P. J. Yoo, C. Y. Chiang, N. Meethong, P. T. Hammond, Y. M. Chiang, and A. M. Belcher, *Science* **312**, 885 (2006).
- <sup>28</sup>Y. J. Lee, H. Yi, W. J. Kim, K. Kang, D. S. Yun, M. S. Strano, G. Ceder, and A. M. Belcher, *Science* **324**, 1051 (2009).
- <sup>29</sup>Y. J. Lee and A. M. Belcher, *J. Mater. Chem.* **21**, 1033 (2011).
- <sup>30</sup>D. Y. Oh, X. N. Dang, H. J. Yi, M. A. Allen, K. Xu, Y. J. Lee, and A. M. Belcher, *Small* **8**, 1006 (2012).
- <sup>31</sup>J. N. Culver, A. D. Brown, F. H. Zang, M. Gnerlich, K. Gerasopoulos, and R. Ghodssi, *Virology* **479**, 200 (2015).
- <sup>32</sup>K. T. Nam, R. Wartena, P. J. Yoo, F. W. Liau, Y. J. Lee, Y. M. Chiang, P. T. Hammond, and A. M. Belcher, *Proc. Natl. Acad. Sci. U. S. A.* **105**, 17227 (2008).
- <sup>33</sup>B. L. Adams, A. S. Finch, M. M. Hurley, D. A. Sarkes, and D. N. Stratidis-Cullum, *Adv. Mater.* **25**, 4585 (2013).
- <sup>34</sup>M. Sarikaya, C. Tamerler, A. K. Y. Jen, K. Schulten, and F. Baneyx, *Nat. Mater.* **2**, 577 (2003).
- <sup>35</sup>H. de Haard, P. Henderikx, and H. R. Hoogenboom, *Adv. Drug Deliv. Rev.* **31**, 5 (1998).
- <sup>36</sup>H. R. Hoogenboom, A. P. de Bruine, S. E. Hufton, R. M. Hoet, J. W. Arends, and R. C. Roovers, *Immunotechnology* **4**, 1 (1998).
- <sup>37</sup>S. Brown, *Proc. Natl. Acad. Sci.* **89**, 8651 (1992).
- <sup>38</sup>S. Brown, M. Sarikaya, and E. Johnson, *J. Mol. Biol.* **299**, 725 (2000).
- <sup>39</sup>J. M. Slocik, R. R. Naik, M. O. Stone, and D. W. Wright, *J. Mater. Chem.* **15**, 749 (2005).
- <sup>40</sup>R. R. Naik, S. E. Jones, C. J. Murray, J. C. McAuliffe, R. A. Vaia, and M. O. Stone, *Adv. Funct. Mater.* **14**, 25 (2004).
- <sup>41</sup>M. Umetsu, M. Mizuta, K. Tsumoto, S. Ohara, S. Takami, H. Watanabe, I. Kumagai, and T. Adschariri, *Adv. Mater.* **17**, 2571 (2005).
- <sup>42</sup>R. R. Naik, L. L. Brott, S. J. Clarkson, and M. O. Stone, *J. Nanosci. Nanotechnol.* **2**, 95 (2002).
- <sup>43</sup>Y. Fang, N. Poulsen, M. B. Dickerson, Y. Cai, S. E. Jones, R. R. Naik, N. Kroger, and K. H. Sandhage, *J. Mater. Chem.* **18**, 3871 (2008).
- <sup>44</sup>S. R. Whaley, D. S. English, E. L. Hu, P. F. Barbara, and A. M. Belcher, *Nature* **405**, 665 (2000).
- <sup>45</sup>C. B. Mao, C. E. Flynn, A. Hayhurst, R. Sweeney, J. F. Qi, G. Georgiou, B. Iverson, and A. M. Belcher, *Proc. Natl. Acad. Sci. U. S. A.* **100**, 6946 (2003).
- <sup>46</sup>C. F. Barbas, A. S. Kang, R. A. Lerner, and S. J. Benkovic, *Proc. Natl. Acad. Sci. U. S. A.* **88**, 7978 (1991).
- <sup>47</sup>J. L. Allen, T. Thompson, J. Sakamoto, C. R. Becker, T. R. Jow, and J. Wolfenstine, *J. Power Sources* **254**, 204 (2014).
- <sup>48</sup>J. Ludwig and T. Nilges, *J. Power Sources* **382**, 101 (2018).
- <sup>49</sup>X. Y. Feng, C. Shen, X. Fang, and C. H. Chen, *J. Alloys Compd.* **509**, 3623 (2011).
- <sup>50</sup>E. Hosono, T. Kudo, I. Honma, H. Matsuda, and H. S. Zhou, *Nano Lett.* **9**, 1045 (2009).
- <sup>51</sup>R. Benedek, M. M. Thackeray, and A. van de Walle, *Chem. Mater.* **20**, 5485 (2008).
- <sup>52</sup>I. A. Shkrob, J. A. Gilbert, P. J. Phillips, R. Klie, R. T. Haasch, J. Barenco, and D. P. Abraham, *J. Electrochem. Soc.* **164**, A1489 (2017).
- <sup>53</sup>K. I. Sano, H. Sasaki, and K. Shiba, *Langmuir* **21**, 3090 (2005).
- <sup>54</sup>M. Ploss, S. J. Facey, C. Bruhn, L. Zemel, K. Hofmann, R. W. Stark, B. Albert, and B. Hauer, *BMC Biotechnol.* **14**, 12 (2014).
- <sup>55</sup>R. Derda, S. K. Y. Tang, S. C. Li, S. Ng, W. Matochko, and M. R. Jafari, *Molecules* **16**, 1776 (2011).
- <sup>56</sup>D. Rothenstein, B. Claasen, B. Omiecienski, P. Lammel, and J. Bill, *J. Am. Chem. Soc.* **134**, 12547 (2012).
- <sup>57</sup>See supplementary material at <https://doi.org/10.1116/1.5111735> for a phage display schematic, zeta potential measurements of particles, table of all identified SBPs, and control TEM images of particles.